DEUTSCHES ELEKTRONEN-SYNCHROTRON DESY

DESY 87-089
August 1987

SUPERSYMMETRY IN ep COLLISIONS

by

H. Komatsu and R. Rückl

Deutsches Elektronen-Synchrotron DESY, Hamburg

ISSN 0418-9833

NOTKESTRASSE 85 · 2 HAMBURG 52

To be sure that your preprints are promptly included in the
HIGH ENERGY PHYSICS INDEX ,
send them to the following address (if possible by air mail) :

DESY
Bibliothek
Notkestrasse 85
2 Hamburg 52
Germany

DESY 87-089
August 1987

ISSN 0418-9833

SUPERSYMMETRY IN EP COLLISIONS

H. Komatsu*+ and R. Rückl

Deutsches Elektronen-Synchrotron DESY, Hamburg

Contribution to the Workshop on Physics at Future Accelerator,
La Thuile and CERN, 1987

* Present address: Institut für Physik, Universität Dortmund,
D-4600 Dortmund 50, Fed. Rep. Germany

+ Supported by the Deutsche Forschungsgemeinschaft

SUPERSYMMETRY IN EP COLLISIONS

H.Komatsu*+ and R. Rückl
Deutsches Elektronen-Synchrotron DESY, Hamburg, Fed. Rep. of Germany

ABSTRACT

We study the production of supersymmetric particles in ep collisions which would be provided by LEP and LHC operating in the ep mode. The following final states have been considered: $e\tilde{e}\tilde{q}$ + X, $\tilde{\nu}\tilde{q}$ + X, $eq\bar{\tilde{q}}$ + X, $eq\tilde{g}$ + X and $e\tilde{\gamma}$ + X. The discovery potential of this ep option is estimated in terms of detection limits for sparticle masses.

1. INTRODUCTION

In the minimal supersymmetric extension of the standard model with two scalar Higgs doublets [1], one expects the following superpartners: spin 0 sleptons ($\tilde{l}_{L,R}$) and squarks ($\tilde{q}_{L,R}$) associated with the L- and R-handed leptons and quarks, spin 1/2 gluinos ($\tilde{g}$) and electroweak gauginos ($\tilde{\gamma}$, $\tilde{Z}$, $\tilde{W}^{\pm}$) associated with the gluons and the photon, Z and $W^{\pm}$ bosons, respectively, and spin 1/2 higgsinos ($\tilde{H}_1^0$, $\tilde{H}_1^-$, $\tilde{H}_2^+$, $\tilde{H}_2^0$) associated with the Higgs bosons. The couplings of these new fields are related by supersymmetry to the familiar gauge and Yukawa couplings of the ordinary standard model. The breaking of $SU(2)_L \times U(1)$ and supersymmetry induces mixings among superpartners with the same $SU(3)_c \times U(1)_{em}$ quantum numbers and generates masses. Possible dynamical schemes for symmetry breaking are suggested by supergravity models [1].

High-energy electron-proton machines providing, effectively, collisions of electrons and (virtual) vector bosons with quarks, gluons and (virtual) vector bosons open several ways to search for supersymmetric particles. The possibility to pair-produce

- sleptons and squarks [2-4]: $eq \to e\tilde{q}$, $\tilde{\nu}\tilde{q}$,
- squarks and antisquarks [2,5]: $\gamma g \to \tilde{q}\bar{\tilde{q}}$,
- squarks and gluinos [2,5]: $\gamma q \to \tilde{q}\tilde{g}$,
- sleptons and gauginos [6,7]: $e\gamma \to \tilde{e}(\tilde{\gamma}$ or $\tilde{Z})$, $\tilde{\nu}\tilde{W}$,
- squarks and gauginos: $q\gamma \to \tilde{q}(\tilde{\gamma}$, $\tilde{Z}$ or $\tilde{W})$,

in principle, allows to check the existence of many of the sparticles expected in the supersymmetric standard model. Additional, but less direct evidence may arise from effects of squarks and gluinos on the running of the strong coupling constant $\alpha_s(Q^2)$, and from changes of properties of deep-inelastic structure functions and sum rules due to the evolution of a $\tilde{q}$ and $\tilde{g}$ sea in the proton [8]. However, in view of the current limits on sparticle masses [9], for example,

$$m_{\tilde{e}},\ m_{\tilde{W}} \gtrsim 20 \text{ GeV}, \qquad m_{\tilde{q}},\ m_{\tilde{g}} \gtrsim 60 \text{ GeV}, \tag{1}$$

---

* Present address: Institut für Physik, Universität Dortmund, D-4600 Dortmund 50, FRG
+ Supported by the Deutsche Forschungsgemeinschaft

to quote only the least model-dependent bounds, $\tilde{e}\tilde{q}$, $\tilde{q}\bar{\tilde{q}}$ and $\tilde{q}\tilde{g}$ production seem to offer by far better prospect for discoveries than the other possibilities mentioned above. We shall therefore concentrate on these processes.

The aim of the present study is to calculate the total production cross-sections for $ep \to \tilde{l}\tilde{q}X$, $ep \to e\tilde{q}\bar{\tilde{q}}X$ and $ep \to e\tilde{q}\tilde{g}X$ using various models for sparticle masses, and to estimate discovery limits. The following substitutions have been made in our numerical calculations: set I of ref.[10] with varying evolution scales for the quark distribution functions, $\alpha_s(Q^2) = 4\pi/7\,\ell n(Q^2/(200\ \mathrm{MeV})^2)$ for the running coupling constant of QCD, $\alpha = 1/137$ for the fine structure constant, $\sin^2\Theta_W = 0.23$ for the Weinberg angle and $m_Z = m_W/\cos\Theta_W = 93$ GeV for the masses of the Z and W bosons.

Finally, for most estimates we have assumed the ep c.m. energies and luminosities,

$$\begin{aligned} &\text{(I)}\ \sqrt{s} = 1.4\ \text{TeV and}\ L = 10^{32}\mathrm{cm}^{-2}\mathrm{s}^{-1}\ , \\ &\text{(II)}\ \sqrt{s} = 1.8\ \text{TeV and}\ L = 10^{31}\mathrm{cm}^{-2}\mathrm{s}^{-1}\ , \end{aligned} \tag{2}$$

which could be obtained by colliding an (50-100) GeV electron (or positron) beam of LEP with a 8 TeV proton beam of LHC, the hadron collider in the LEP tunnel. The feasibility and machine parameters of this ep option have been discussed at this workshop [11]. A summary of our main results is given in the report of the physics-2 working group by J. Ellis and F. Pauss [12].

2. SLEPTON-SQUARK PRODUCTION

Sleptons and squarks are pair-produced in ep collisions by t-channel exchanges of gauginos and higgsinos. One has two kinds of processes, the charged-current type processes $eq \to \tilde{\nu}\tilde{q}$ involving $\tilde{W}^{\pm}$, $\tilde{H}_1^-$ and $\tilde{H}_2^+$ exchanges, and the neutral-current type processes $eq \to e\tilde{q}$ involving $\tilde{\gamma}$, $\tilde{Z}$, $\tilde{H}_1^0$ and $\tilde{H}_2^0$ exchanges. As a matter of fact, these are in general not the physical fields which acquire definite masses. The mass eigenstates, called charginos and neutralinos, are rather mixtures of gauginos and higgsinos. Thus, before one can calculate $\tilde{l}\tilde{q}$ production cross-sections, one has to solve the gaugino-higgsino mixing problem. Further complications may arise in the scalar sector due to mixing of the $\tilde{f}_L$ and $\tilde{f}_R$ partners of leptons and quarks. However, in supergravity models [1] this effect is expected to be small, perhaps with the exception of $\tilde{t}_L$ - $\tilde{t}_R$ mixing, and will therefore be neglected. Also flavor mixing is disregarded being essentially irrelevant for the numerical examples we have chosen to study.

2.1 Gaugino-Higgsino Mixing

As a model for gaugino-higgsino mixing [1] we consider the non-diagonal mass matrices

$$M^C = \begin{array}{c|cc|c} & \tilde{W}^+ & \tilde{H}_2^+ & \\ \hline & M_2 & i\sqrt{2}\, m_W \cos\Theta_V & \tilde{W}^- \\ & i\sqrt{2}\, m_W \sin\Theta_V & -\mu & \tilde{H}_1^- \end{array} \tag{3}$$

and

$$M^N = \begin{array}{c|cccc} & \tilde{\gamma} & \tilde{Z} & \tilde{H} & \tilde{H}' \\ \hline \tilde{\gamma} & M_1\cos^2\Theta_W + M_2\sin^2\Theta_W & (M_2 - M_1)\cos\Theta_W\sin\Theta_W & 0 & 0 \\ \tilde{Z} & (M_2 - M_1)\cos\Theta_W\sin\Theta_W & M_1\sin^2\Theta_W + M_2\cos^2\Theta_W & im_Z & 0 \\ \tilde{H} & 0 & im_Z & -\mu\sin 2\Theta_V & \mu\cos 2\Theta_V \\ \tilde{H}' & 0 & 0 & \mu\cos 2\Theta_V & \mu\sin 2\Theta_V \end{array} \qquad (4)$$

where the neutral higgsinos $\tilde{H}$ and $\tilde{H}'$ are linear combinations of the $SU(2)_L$-doublet fields $\tilde{H}^\circ_{1,2}$,

$$\begin{aligned} \tilde{H} &= \cos\Theta_V\, \tilde{H}^\circ_1 - \sin\Theta_V\, \tilde{H}^\circ_2 \quad , \\ \tilde{H}' &= \sin\Theta_V\, \tilde{H}^\circ_1 + \cos\Theta_V\, \tilde{H}^\circ_2 \quad , \end{aligned} \qquad (5)$$

and

$$\tan\Theta_V = \frac{v_2}{v_1} \quad , \qquad (6)$$

v_1 and v_2 being the vacuum expectation values of the two neutral scalar Higgs fields H°_1 and H°_2. The generally complex mass parameters M_1 , M_2 and μ in the above are soft SUSY breaking parameters associated with the U(1) and $SU(2)_L$ gauginos and with the higgsinos, respectively. Furthermore, we assume the constraints

$$\begin{aligned} &\text{(a)}\ \cos 2\Theta_V = 0 \quad , \\ &\text{(b)}\ M_1 = \frac{5}{3}\tan^2\Theta_W\, M_2 \quad , \\ &\text{(c)}\ M_1,\ M_2 \text{ and } \mu \text{ real} \ . \end{aligned} \qquad (7)$$

Assumptions (a) and (b) are suggested by the renormalization group analysis [13] of a class of supergravity models (for a top quark mass $m_t \simeq 50$ GeV), while assumption (c) is made merely for simplicity. With these specifications the model contains only two unknown parameters, M_2 and μ.

The mass matrices (3) and (4) can then be diagonalized by unitary matrices C and N:

$$\begin{aligned} (C^T M^C C)_{ij} &= m_{Ci}\delta_{ij} \quad , \\ (N^T M^N N)_{ij} &= m_{Ni}\delta_{ij} \quad . \end{aligned} \qquad (8)$$

The (positive) eigenvalues m_{Ci} , $i = 1,2$ and m_{Ni} , $i = 1,\ldots, 4$ are the masses of the chargino states

$$\tilde{\chi}_{Ci} = C_{1i}\tilde{W}^- + C_{2i}\tilde{H}^- \ ; \ i = 1,2 \qquad (9)$$

and of the neutralino states

$$\tilde{X}_{Ni} = N_{1i}\tilde{\gamma} + N_{2i}\tilde{Z} + N_{3i}\tilde{H} + N_{4i}\tilde{H}' \; ; \quad i = 1,\ldots, 4, \tag{10}$$

respectively. As a consequence of assumption (7a), the higgsino $\tilde{H}'$ does not get mixed with the other neutral fields so that $N_{4i} = 0$ for $i = 1, 2, 3$ and $\tilde{X}_{N4} = \tilde{H}'$ with $m_{N4} = |\mu|$. Ordering the remaining eigenstates $\tilde{X}_{Ni}$, $i = 1,2,3$ and $\tilde{X}_{Ci}$, $i = 1,2$ such that $m_{N1} \leq m_{N2} \leq m_{N3}$ and $m_{C1} \leq m_{C2}$, we use the physical masses m_{N1} and m_{C1}, instead of M_2 and μ, as input in the diagonalization of M^C and the appropriate 3x3 submatrix of M^N.

The resulting neutralino and chargino states and masses are given in Table 1 for values of m_{N1} and m_{C1} up to O(1 TeV), that is the mass range of interest for the present studies. Also shown in Table 1 are the values of M_2 (with the convention $M_2 \geq 0$) and μ associated with a given solution. A detailed discussion of these mixing scenarios can be found in ref. [4].

2.2 Cross-Sections

Cross-sections for $ep \to \tilde{l}\tilde{q}X$ are calculated from the diagrams indicated in Fig.1. For an incident electron and quark with the same helicity a = L or R one obtains the differential cross-section [2,4]

$$\frac{d\sigma}{d\hat{t}}(e_a^- q_a \to \tilde{l}_a \tilde{q}_a) = \frac{1}{16\pi\hat{s}} \left| \sum_i \frac{(\eta e_a)_i (\eta q_b)_i}{\hat{t} - m_i^2} \; m_i \right|^2 \quad , \tag{11}$$

whereas for opposite helicities a = L, b = R or vice versa one finds [2,4]

$$\frac{d\sigma}{d\hat{t}}(e_a^- q_b \to \tilde{l}_a \tilde{q}_b) = \frac{1}{16\pi\hat{s}^2} \left| \sum_i \frac{(\eta e_a)_i (\eta q_b)_i}{\hat{t} - m_i^2} \right|^2 \times \left[-\hat{t}\hat{s} - (m_{\tilde{l}_a}^2 - \hat{t})(m_{\tilde{q}_b}^2 - \hat{t}) \right] . \tag{12}$$

Here, we use the scattering variables

$$\hat{s} = (p_e + p_q)^2, \; \hat{t} = (p_e - p_{\tilde{l}})^2, \; \hat{u} = (p_e - p_{\tilde{q}})^2 \tag{13}$$

with $\hat{s} + \hat{t} + \hat{u} = m_{\tilde{l}}^2 + m_{\tilde{q}}^2$, $m_{\tilde{l}}$ and $m_{\tilde{q}}$ being the appropriate slepton and squark masses and p

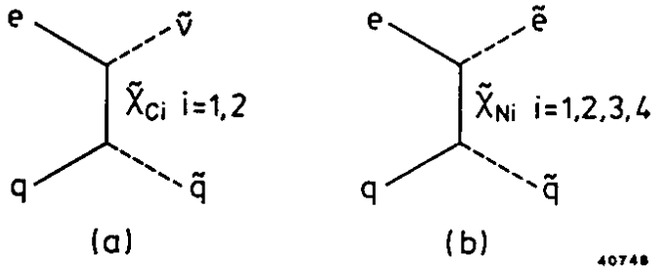

Fig.1 Diagrams contributing to (a) $ep \to \tilde{\nu}\tilde{q}X$ and (b) $ep \to \tilde{e}\tilde{q}X$.

Table 1

Masses and eigenstates of neutralinos and charginos and the corresponding values of the gaugino and higgsino mass parameters M_2 and μ. The values of m_{N1} and m_{C1} are used as input. The neutralino states $\tilde{\chi}_{Ni}$, i = 1,2,3 are characterized by the coefficients N_{ji} of eq.(10) with $N_{4i} = 0$ and $\tilde{\chi}_{N4} = \tilde{H}'$ with $m_{N4} = |\mu|$. The chargino state $\tilde{\chi}_{C1}$ is represented by the coefficients C_{j1} of eq.(9), while the coefficients C_{j2} of the state $\tilde{\chi}_{C2}$ are given by $C_{12} = -i\,\varepsilon\, C_{21}\,|C_{11}|/C_{11}$ and $C_{22} = -i\,\varepsilon\,|C_{11}|$ with $\varepsilon = 1$ for $M_2 + \mu > 0$ and $\varepsilon = i$ for $M_2 + \mu < 0$.

Neutralinos			Charginos		SUSY breaking	
$m_{N1}\,(N_{11}, N_{21}, N_{31})$	$m_{N2}\,(N_{12}, N_{22}, N_{32})$	$m_{N3}\,(N_{13}, N_{23}, N_{33})$	$m_{C1}\,(C_{11}, C_{21})$	m_{C2}	M_2	μ
0(1.000 , 0.0 , 0.0)	38(0.000 ,-0.927i, 0.375)	230(0.000 , 0.375 ,-0.927i)	30(0.939i,-0.345)	222	0.0	192.0
0(1.000 , 0.0 , 0.0)	60(0.000 , 0.839 ,-0.544i)	143(0.000 ,-0.544i, 0.839)	50(0.853 ,-0.522i)	133	0.0	-83.2
0(1.000 , 0.0 , 0.0)	91(0.000 , 0.713 ,-0.701i)	95(0.000 ,-0.701i, 0.713)	80(0.714 ,-0.700i)	83	0.0	-3.2
20(0.103 ,-0.277 ,-0.955i)	221(0.895 ,-0.393 , 0.210i)	441(0.434 , 0.877 ,-0.207i)	30(0.203 , 0.979i)	441	423.7	46.9
20(0.996 , 0.047 , 0.077i)	44(0.084i,-0.790i, 0.607)	149(0.032 , 0.611 ,-0.791i)	30(0.796i,-0.605)	139	32.1	77.3
20(0.972 ,-0.231 , 0.050i)	52(0.237 , 0.952 ,-0.192i)	429(0.003i,-0.198i, 0.980)	50(0.985 ,-0.175i)	424	35.5	-410.0
20(0.997 , 0.009 , 0.074i)	64(0.058i,-0.711i, 0.701)	123(0.047 , 0.703 ,-0.709i)	50(0.703i,-0.711)	113	32.5	30.7
20(0.996 ,-0.061 , 0.069i)	88(0.089 , 0.847 ,-0.524i)	120(0.026i,-0.528i, 0.849)	80(0.868 ,-0.497i)	109	33.3	-62.7
20(0.997 ,-0.032 , 0.072i)	92(0.038i,-0.608i, 0.793)	101(0.069 , 0.793 ,-0.605i)	80(0.586i,-0.811)	92	33.0	-21.0
50(0.982 ,-0.089 , 0.164i)	64(0.087i,-0.563i, 0.822)	140(0.166 , 0.822 ,-0.545i)	50(0.520i,-0.854)	134	84.1	-0.4
50(0.374 ,-0.635 ,-0.676i)	123(0.898 , 0.066 , 0.436i)	258(0.232 , 0.770 ,-0.595i)	80(0.575 , 0.818i)	253	196.1	137.4
50(0.978 ,-0.145 , 0.150i)	92(0.061i,-0.488i, 0.870)	131(0.200 , 0.860 ,-0.469i)	80(0.441i,-0.897)	126	85.9	-39.9
50(0.872 ,-0.490 ,-0.008i)	100(0.490 , 0.872 , 0.014i)	6103(0.000 , 0.015 ,-1.000i)	100(1.000 , 0.014i)	6103	101.1	6102.0
50(0.974 ,-0.175 , 0.142i)	111(0.050i,-0.447i, 0.893)	127(0.219 , 0.877 ,-0.427i)	100(0.400i,-0.916)	123	86.9	-64.4
100(0.931 ,-0.323 , 0.170i)	109(0.058i,-0.329i, 0.942)	210(0.361 , 0.887 ,-0.288i)	100(0.275i,-0.961)	209	185.2	-76.6
100(0.582 ,-0.624 ,-0.521i)	175(9.775 , 0.231 , 0.589i)	324(0.247 , 0.746 ,-0.618i)	150(0.601 , 0.799i)	320	258.5	211.4
100(0.924 ,-0.354 , 0.143i)	157(0.041i,-0.281i, 0.959)	209(0.379 , 0.892 ,-0.245i)	150(0.235i,-0.972)	208	187.8	-130.3
100(0.872 ,-0.489 ,-0.014i)	200(0.490 , 0.872 , 0.026i)	3317(0.000 , 0.030 ,-1.000i)	200(1.000 , 0.026i)	3316	202.1	3314.1
100(0.919 ,-0.375 , 0.123i)	206(0.030i,-0.244i, 0.969)	208(0.393 , 0.894 ,-0.213i)	200(0.205i,-0.979)	207	189.7	-182.9
200(0.893 ,-0.437 , 0.105i)	205(0.032i,-0.171i, 0.985)	404(0.449 , 0.883 ,-0.139i)	200(0.136i,-0.991)	404	392.3	-188.8
200(0.760 ,-0.552 ,-0.343i)	314(0.561 , 0.292 , 0.775i)	486(0.327 , 0.782 ,-0.531i)	300(0.518 , 0.855i)	484	434.7	349.4
200(0.891 ,-0.446 , 0.085i)	304(0.022i,-0.144i, 0.989)	404(0.454 , 0.883 ,-0.118i)	300(0.117i,-0.993)	404	394.1	-290.4
200(0.873 ,-0.488 ,-0.023i)	400(0.488 , 0.871 , 0.047i)	2139(0.002 , 0.052 ,-0.999i)	400(0.999 , 0.047i)	2138	403.8	2133.9
200(0.889 ,-0.452 , 0.071i)	403(0.016i,-0.124i, 0.992)	404(0.457 , 0.883 ,-0.103i)	400(0.102i,-0.995)	404	395.4	-391.6
400(0.882 ,-0.469 , 0.055i)	402(0.016i,-0.086i, 0.996)	804(0.472 , 0.879 ,-0.068i)	400(0.068i,-0.998)	804	798.6	-394.4
400(0.840 ,-0.504 ,-0.204i)	609(0.347 , 0.209 , 0.914i)	853(0.418 , 0.838 ,-0.350i)	600(0.345 , 0.939i)	852	822.1	630.0
400(0.881 ,-0.471 , 0.044i)	602(0.011i,-0.072i, 0.997)	804(0.473 , 0.879 ,-0.058i)	600(0.058i,-0.998)	804	799.5	-595.2
400(0.874 ,-0.485 ,-0.031i)	800(0.486 , 0.871 , 0.076i)	1877(0.010 , 0.081 ,-0.997i)	800(0.997 , 0.076i)	1875	806.2	1869.2
400(0.880 ,-0.473 , 0.037i)	802(0.008i,-0.062i, 0.998)	804(0.474 , 0.879 ,-0.051i)	800(0.051i,-0.999)	804	800.2	-795.8
800(0.879 ,-0.477 , 0.028i)	801(0.008i,-0.043i, 0.999)	1607(0.478 , 0.878 ,-0.034i)	800(0.034i,-0.999)	1607	1604.5	-797.2
800(0.867 ,-0.486 ,-0.109i)	1205(0.188 , 0.117 , 0.975i)	1633(0.461 , 0.866 ,-0.193i)	1200(0.192 , 0.981i)	1633	1616.8	1216.0
800(0.878 ,-0.477 , 0.022i)	1201(0.006i,-0.036i, 0.999)	1607(0.478 , 0.878 ,-0.029i)	1200(0.029i,-1.000)	1607	1605.0	-1197.6
800(0.876 ,-0.482 ,-0.030i)	1600(0.482 , 0.868 , 0.117i)	2301(0.030 , 0.117 ,-0.993i)	1600(0.993 , 0.117i)	2300	1609.7	2289.9
800(0.878 ,-0.478 , 0.019i)	1601(0.004i,-0.031i, 1.000)	1607(0.478 , 0.878 ,-0.025i)	1600(0.025i,-1.000)	1607	1605.3	-1597.9

40776

denoting particle four-momenta. The effective couplings $(\eta_{f_c})_i$ are given by

$$(\eta_{f_L})_i^C = \frac{e}{\sin\Theta_W} C_{1i}, \quad (\eta_{f_R})_i^C = 0 \tag{14}$$

in the charged-current case $\tilde{l} = \tilde{\nu}$, and by

$$(\eta_{f_L})_i^N = \sqrt{2}\, e \left[Q_f N_{1i} + \frac{T_{3f} - Q_f \sin^2\Theta_W}{\sin\Theta_W \cos\Theta_W} N_{2i}\right]$$

$$(\eta_{f_R})_i^N = \sqrt{2}\, e\, Q_f \left[N^*_{1i} - \tan\Theta_W N^*_{2i}\right] \tag{15}$$

in the neutral-current case $\tilde{l} = \tilde{e}$. Moreover, Q_f denotes the electromagnetic charge (with the convention of $Q_e = -1$), T_{3f} is the third component of the weak isospin, and C_{1i}, N_{1i} and N_{2i} are elements of the diagonalization matrices introduced in eq.(8) describing the wino, photino and zino admixtures in the chargino and neutralino eigenstates (see eqs.(9) and (10)). Since the higgsino Yukawa couplings vanish in the limit m_e, $m_q \to 0$, an approximation made throughout this paper, the higgsino contributions proportional to C_{2i}, N_{3i} and N_{4i} are dropped in eqs.(14) and (15). Finally, the polarized differential cross-sections for the processes $e^-_a\bar{q}_b \to \tilde{l}_a\bar{\tilde{q}}_{b'}$, $e^+_a q_b \to \bar{\tilde{l}}_{a'}\tilde{q}_b$ and $e^+_a\bar{q}_b \to \bar{\tilde{l}}_{a'}\bar{\tilde{q}}_{b'}$ can be obtained from $d\sigma(e^-_a q_b \to \tilde{l}_a\tilde{q}_b)/d\hat{t}$ by the following replacements

$$\begin{aligned} (\eta_{f_L})_i &\to (\eta_{f_R})_i^* \quad \text{for } f_L \to \bar{f}_L \quad , \\ (\eta_{f_R})_i &\to (\eta_{f_L})_i^* \quad \text{for } f_R \to \bar{f}_R \quad . \end{aligned} \tag{16}$$

In our notation, $\bar{\tilde{f}}_R$ and $\bar{\tilde{f}}_L$ denote the scalar partners of $\bar{f}_L$ and $\bar{f}_R$ so that in the above $a' = L,R$ is associated with $a = R,L$ (similarly, for b and b').

In the next paragraph, we present numerical predictions for the total unpolarized production cross-sections

$$\sigma(ep \to \tilde{l}\tilde{q}X) = \sum_{a,b} \sum_{q} \int_{x_{min}}^{1} dx \int_{t_{max}}^{t_{min}} d\hat{t}\, \frac{1}{4} \frac{d\sigma(e_a q_b \to \tilde{l}_a \tilde{q}_b)}{d\hat{t}} \quad q(x,Q^2) \tag{17}$$

where the integration boundaries are given by

$$\begin{aligned} x_{min} &= (m_{\tilde{l}_a} + m_{\tilde{q}_b})^2/s \quad , \\ t^{min}_{max} &= -\frac{1}{2}\left(sx - m^2_{l_a} - m^2_{q_b} \mp \sqrt{(sx - m^2_{\tilde{l}_a} - m^2_{\tilde{q}_b})^2 - 4m^2_{\tilde{l}_a} m^2_{\tilde{q}_b}}\right) \quad . \end{aligned} \tag{18}$$

The factor $\frac{1}{4}$ in eq.(17) arises from averaging over the incident lepton (e^- or e^+) and quark polarizations. For the evolution scale of the quark (and antiquark) distribution functions $q(x, Q^2)$ we choose, somewhat arbitrarily, $Q^2 = -\hat{t}$. Furthermore, we sum over all flavors present in the proton and add the cross-sections for the final states $\tilde{l}_a\,\tilde{q}_b$ with $a,b \in \{L,R\}$.

2.3 Numerical Results

The following numerical examples illustrate pair-production of sleptons and squarks for chargino and neutralino spectra taken from Table 1. As far as the scalar masses are concerned, we have studied three cases: $m_{\tilde{l}} \simeq m_{\tilde{q}}$, $m_{\tilde{l}} \ll m_{\tilde{q}}$, and $m_{\tilde{l}}$ and $m_{\tilde{q}}$ as given by the renormalization group relations of a supergravity model.

2.3.1 $\sigma(ep \to \tilde{l}\tilde{q}X)$ for $m_{\tilde{l}} \simeq m_{\tilde{q}}$

Fig.2 shows the $\tilde{l}\tilde{q}$ production cross-sections versus $m_{\tilde{l}} + m_{\tilde{q}}$ for $m_{\tilde{l}_L} = m_{\tilde{l}_R} = m_{\tilde{q}_L} = m_{\tilde{q}_R}$ and for the gaugino-higgsino mixing scenarios indicated below:

	m_{N1}	m_{C1}	M_2	μ	in GeV
(a)	20	50	36	-410	
(b)	50	100	87	- 64	
(c)	100	200	202	3314	
(d)	200	300	435	349	
(e)	400	600	822	630	

(19)

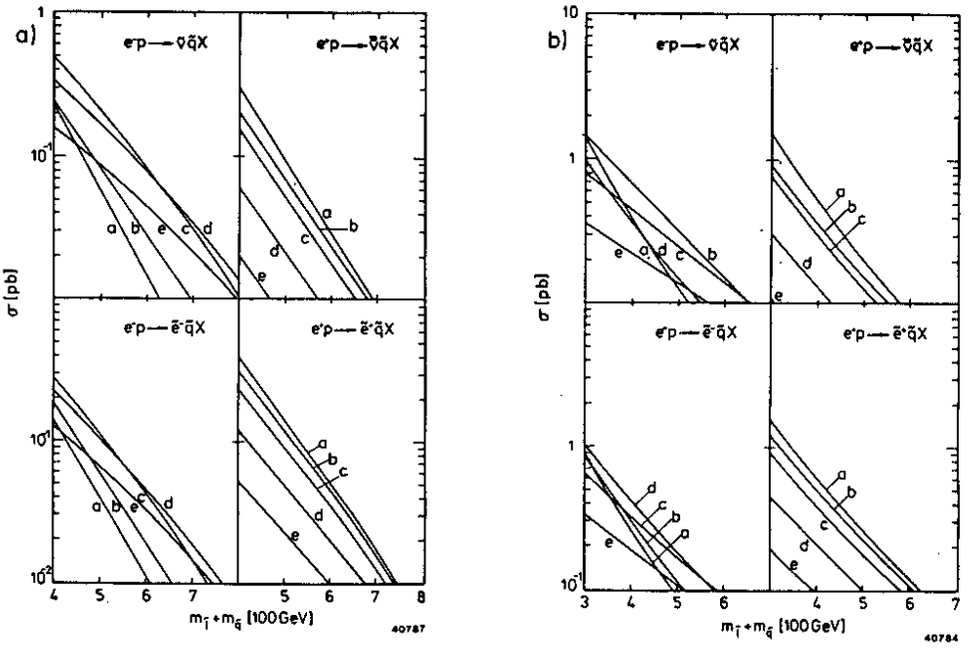

Fig.2 Slepton-squark production cross-sections at (a) $\sqrt{s}$ = 1.4 TeV and (b) $\sqrt{s}$ = 1.8 TeV assuming $m_{\tilde{l}} = m_{\tilde{q}}$ and using models (a)-(e) of (19) for the chargino and neutralino states.

The full $\tilde{\chi}_{Ci}$ and $\tilde{\chi}_{Ni}$ spectra for the cases (a)-(e) can be found in Table 1. These examples demonstrate a great sensitivity of the cross-sections to the chargino and neutralino models. It is interesting to note that the relative magnitude of the e^+p cross-sections follows the pattern one would naively expect from the masses m_{N1} and m_{C1} of the lightest states, while the e^-p cross-sections exhibit a more irregular behaviour due to a subtle interplay of valence and sea quark contributions. Furthermore, although we have taken $m_{\tilde{l}} = m_{\tilde{q}}$ in the calculation, the results plotted in Fig.2 also apply to cases $m_{\tilde{l}} \neq m_{\tilde{q}}$ as long as the slepton and squark masses are not too different. The point is that integrated cross-sections receive the dominant contributions from the region $x \simeq x_{min} = (m_{\tilde{l}} + m_{\tilde{q}})^2/s$ (see eqs.(17) and (18)) and thus depend, to a rather good approximation, only on the sum $m_{\tilde{l}} + m_{\tilde{q}}$.

We shall now use Fig.2 to estimate detection limits being aware of doing something slightly illegal. One would clearly need more detailed Monte Carlo studies of the dominant $\tilde{l}$ and $\tilde{q}$ decays in the background of standard model processes in order to draw definite conclusions. Such studies are presently only available for $\tilde{l}\tilde{q}$ production and decay at HERA [14]. For the case $ep \to \tilde{e}\tilde{q}X$, $\tilde{e} \to e\tilde{\gamma}$ and $\tilde{q} \to q\tilde{\gamma}$ where the photino is assumed to be massless and stable, it was concluded that 10 events per year are sufficient for detection. This implies a minimum observable cross-section of 0.1 pb at the HERA luminosity $L = 10^{31}cm^{-2}s^{-1}$, provided $\tilde{e} \to e\tilde{\gamma}$ and $\tilde{q} \to q\tilde{\gamma}$ are indeed the dominant decay modes. This result provides some justification for taking $\sigma(ep \to \tilde{e}\tilde{q}X) \simeq 0.01(0.1)$ pb as the discovering limits in ep collisions at $\sqrt{s} = 1.4$ (1.8) TeV and $L = 10^{32}(10^{31})cm^{-2}s^{-1}$. Making the above assumption, we find from Fig.2 that the following sparticle masses can be reached:

$$\begin{aligned} m_{\tilde{e}} \simeq m_{\tilde{q}} &\simeq (360\text{-}380)\ \text{GeV} \quad \text{at } \sqrt{s} = 1.4\ \text{TeV},\ L = 10^{32}cm^{-2}s^{-1}, \\ m_{\tilde{e}} \simeq m_{\tilde{q}} &\simeq (260\text{-}310)\ \text{GeV} \quad \text{at } \sqrt{s} = 1.8\ \text{TeV},\ L = 10^{31}cm^{-2}s^{-1}. \end{aligned} \tag{20}$$

Interestingly, mixing scenarios for which the $\tilde{e}^-\tilde{q}$ production is small, the $\tilde{e}^+\tilde{q}$ production is relatively large, and vice versa. That explains why the detection limits, eq.(20), are almost the same for the different chargino and neutralino spectra considered in Fig.2. Also, for some models $\tilde{\nu}\tilde{q}$ production is more abundant than $\tilde{e}\tilde{q}$ production. On the other hand, $\tilde{\nu}\tilde{q}$ final states may be more difficult to detect than $\tilde{e}\tilde{q}$ events [14] and hence we do not take advantage of this fact in our estimates. Finally, it should be stressed that the higher luminosity of ep collisions at 1.4 TeV more than compensates for the lower energy when compared to the capabilities of the 1.8 TeV option.

2.3.2 $\sigma(ep \to \tilde{l}\tilde{q}X)$ for $m_{\tilde{l}} \ll m_{\tilde{q}}$

We have also considered the possibility that sleptons may be much lighter than squarks. The production cross-sections for $m_{\tilde{l}_L} = m_{\tilde{l}_R} \ll m_{\tilde{q}_L} = m_{\tilde{q}_R}$ and the same gaugino-higgsino models (19) as in the previous study are shown in Fig.3. One sees that even in this extreme case the cross-sections do not differ drastically in the main features from what we have found for $m_{\tilde{l}} = m_{\tilde{q}}$, except that they are generally somewhat larger than the ones obtained in Fig.2. This means that one can reach very heavy squark if the sleptons

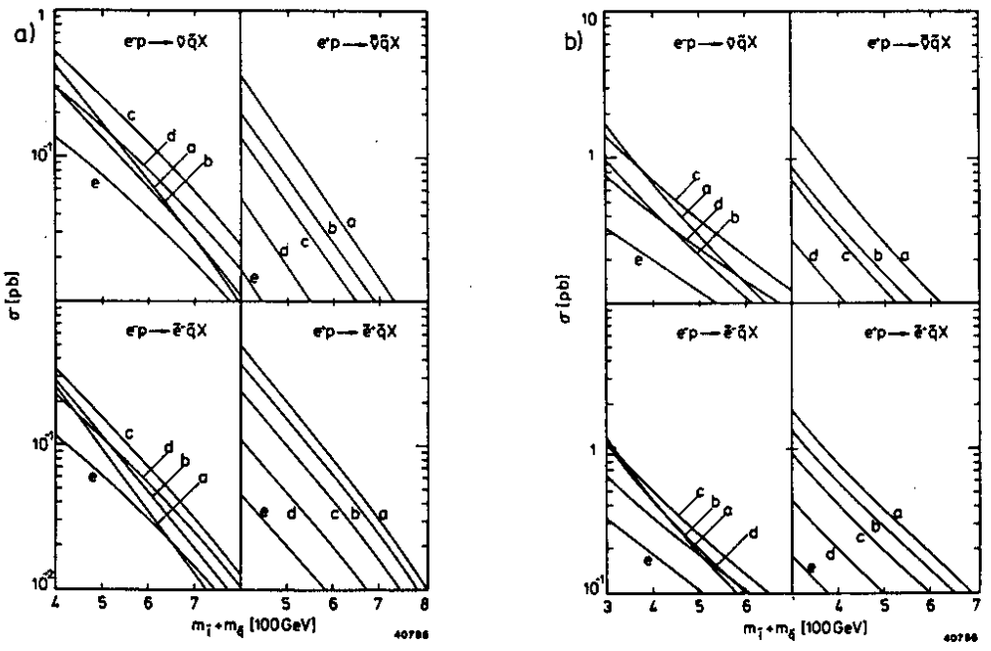

Fig. 3 Same as Fig.2 for $m_{\tilde{l}} = 50$ GeV $\ll m_{\tilde{q}}$.

are light. Taking $m_{\tilde{l}_L} = m_{\tilde{l}_R} = 50$ GeV and estimating the detection limits for sparticle masses under the assumptions which led to eq.(20), we find

$$m_{\tilde{q}} \simeq (700\text{-}770)\ \text{GeV at } \sqrt{s} = 1.4\ \text{TeV},\ L = 10^{32}\text{cm}^{-2}\text{s}^{-1}\ , \qquad (21)$$
$$m_{\tilde{q}} \simeq (450\text{-}630)\ \text{GeV at } \sqrt{s} = 1.8\ \text{TeV},\ L = 10^{31}\text{cm}^{-2}\text{s}^{-1}\ .$$

Again, the ep option with the lower energy but higher luminosity is clearly preferred.

2.3.3 Discovery limits in the framework of a supergravity model

In minimal supergravity models, the $SU(3)_c \times SU(2)_L \times U(1)$ gaugino mass parameters M_3, M_2 and M_1 are related by renormalization group equations to a bare SUSY breaking gaugino mass $m_{1/2}$. Assuming $M_3 = M_2 = M_1 = m_{1/2}$ at a grand-unification scale M_X and evoluting M_i to a scale $Q < M_X$, one obtains

$$m_{1/2}/g_X^2 = M_3/g_3^2(Q) = M_2/g_2^2(Q) = 3\,M_1/5\,g_1^2(Q) \qquad (22)$$

where g_X is the unified gauge coupling at M_X and g_3, g_2 and g_1 denote the usual $SU(3)_c$, $SU(2)_L$ and $U(1)$ gauge couplings, respectively. For $g_X^2/4\pi \simeq 1/24$ at $M_X \simeq 2.4 \cdot 10^{16}$GeV and $\alpha(m_W) = 1/128$, $\sin^2\Theta_W = 0.23$ and $\alpha_s(m_W) \simeq 0.12$, eq.(22) yields [12,13]

$$M_3 \simeq 2.9\, m_{1/2} \quad \text{and} \quad M_1 = \frac{5}{3} \tan^2\Theta_W\, M_2 \simeq 0.41\, m_{1/2} \tag{23}$$

at energy scales of $O(m_W)$. M_2 and M_1 enter the chargino and neutralino mass matrices given in eqs.(3) and (4), while M_3 is the effective gluino mass $m_{\tilde{g}}$. In addition, one also has renormalization group relations for scalar masses. For equal Higgs vacuum expectation values $v_1 = v_2$ as assumed in (7), these relations are approximately given by [12,13]

$$\begin{aligned} m^2_{\tilde{l}_L} &\simeq m_o^2 + 0.5\, m^2_{1/2}, \quad m^2_{\tilde{l}_R} \simeq m_o^2 + 0.15\, m^2_{1/2}, \\ m^2_{\tilde{q}_L} &\simeq m^2_{\tilde{q}_R} \simeq m_o^2 + 7\, m^2_{1/2}, \end{aligned} \tag{24}$$

where the scalar mass parameter m_o defined at M_X is the gravitino mass. Contributions from Yukawa couplings, which mainly affect $m_{\tilde{t}}$, are neglected.

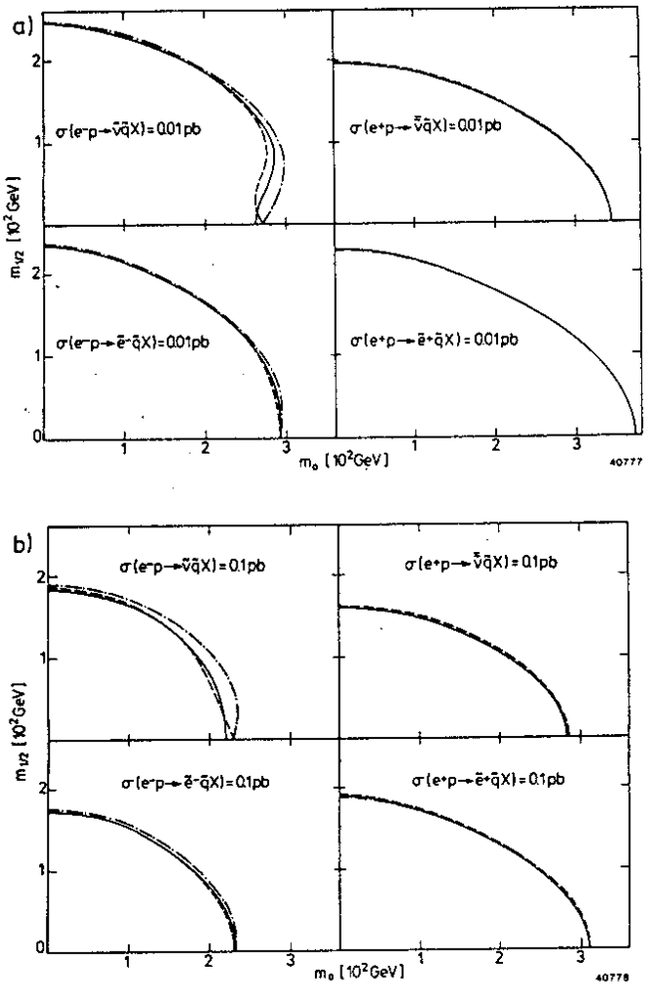

Fig.4 Discovery limits in terms of the parameters $m_{1/2}$ and m_o of a minimal supergravity model. The curves correspond to 10 events per year at (a) $\sqrt{s}$ = 1.4 TeV and (b) $\sqrt{s}$ = 1.8 TeV assuming μ = -100 GeV (dashed-dotted), 0 (full), 100 GeV (dashed).

Within the above model, the chargino and neutralino masses and eigenstates are determined by two bare parameters $m_{1/2}$ and μ, while the scalar masses are given in terms of $m_{1/2}$ and m_o. Hence, the significance of searches for $ep \to \tilde{l}\tilde{q}X$ can be described by limits in the $(m_{1/2}, m_o)$-plane with μ as an additional variable. Fig.4 summarizes our estimates of the region in $(m_{1/2}, m_o)$ which can be explored at $\sqrt{s}$ = 1.4 TeV, $L = 10^{32} cm^{-2} s^{-1}$ and $\sqrt{s}$ = 1.8 TeV, $L = 10^{31} cm^{-2} s^{-1}$. In ref. [12], these limits are compared with constraints expected from SUSY searches in e^+e^- (CLIC) and pp (LHC) collisions, and with the current bounds implying

$$m_{1/2} \gtrsim 55 \text{ GeV} \quad \text{for } m_o \simeq 0 \quad , \qquad (25)$$
$$m_{1/2} \gtrsim 20 \text{ GeV} \quad \text{for } m_o \gtrsim 55 \text{ GeV} \; .$$

One should, however, bear in mind the model-dependence of such a comparison.

2.3.4 Energy-dependence of $\tilde{l}\tilde{q}$-production

We conclude the discussion of $\tilde{l}\tilde{q}$ production with a brief look at the rise of the cross-sections with the ep collision energy. The parameters of the examples illustrated in Fig.5 are as follows:

	m_{N1}	m_{C1}	M_2	μ	$m_{\tilde{l}}$	$m_{\tilde{q}}$	in GeV
a	20	50	33	31	50	100	
b	50	100	87	- 64	100	250	(26)
c	100	200	190	-183	150	600	

with the chargino and neutralino spectra (a)-(c) fully specified in Table 1. The slepton and squark masses are chosen such that they are roughly consistent with the supergravity relations eqs.(23) and (24) for $m_{1/2} \simeq$ 40, 100, 230 GeV and $m_o \simeq$ 40,. 70, 100 GeV in the

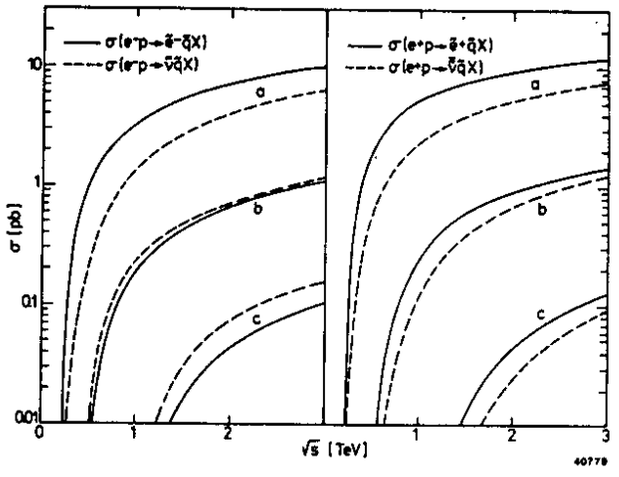

Fig.5 Energy-dependence of slepton-squark production for the models (a)-(c) specified in (26).

cases (a,b,c), respectively. Fig.5 shows the enormous gain in discovery potential by going from the HERA energy range $\sqrt{s} \approx 300$ GeV to TeV energies.

3. SQUARK PRODUCTION

The dominant production mechanism for $\tilde{q}\bar{\tilde{q}}$ pairs at an ep collider is the photon-gluon fusion process described by the diagrams in Fig.6. The integrated cross-section for $\gamma g \to \tilde{q}\bar{\tilde{q}}$ (summed over $\tilde{q}_L$ and $\tilde{q}_R$ with $m_{\tilde{q}_L} = m_{\tilde{q}_R}$) is given by [5]*

$$\sigma(\hat{s}) = \frac{\pi\alpha Q_q^2 \alpha_s(Q^2)}{\hat{s}} \left[2(2+\beta^2) - (1-\beta^4)\, \ell n \frac{1+\beta}{1-\beta}\right] \tag{27}$$

where $\beta = (1 - 4m_q^2/\hat{s})^{1/2}$ and $\hat{s} = (p_\gamma + p_g)^2$. Since the main contribution to the total ep cross-section comes from (almost) real photons radiated off the electron, p_γ^2 is set to zero in eq.(27). Accordingly, the total cross-section for $ep \to e\tilde{q}\bar{\tilde{q}}X$ can be evaluated in the Weizsäcker-Williams approximation (WWA) which, for the case at hand, leads to

$$\sigma(ep \to e\tilde{q}\bar{\tilde{q}}X) = \int_{x_{min}}^{1} dx \int_{z_{min}}^{1} dz\, f_{\gamma/e}(z,q^2)\, G(x,Q^2)\, \sigma(xzs) \tag{28}$$

with

$$z_{min} = (m_1 + m_2)^2/xs, \qquad x_{min} = (m_1 + m_2)^2/s \ , \tag{29}$$

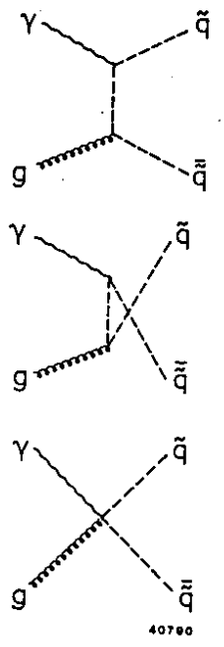

Fig.6 Diagrams contributing to $ep \to e\tilde{q}\bar{\tilde{q}}X$.

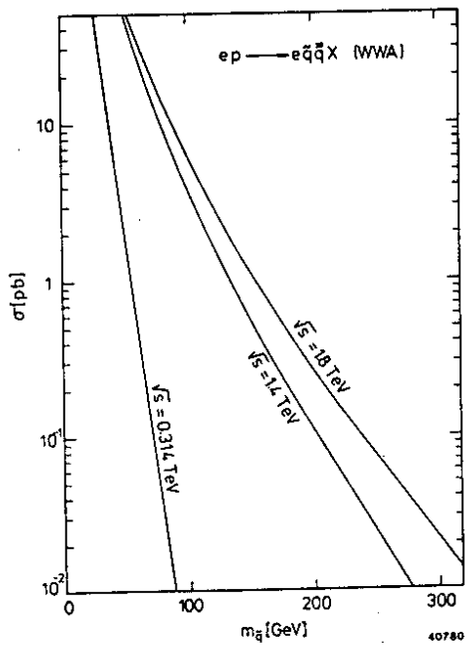

Fig.7 Squark production cross-sections at LEP-LHC and HERA.

* Our result seems to differ by a factor 2 from the cross-section quoted in ref. [5].

and $m_1 = m_2 = m_{\tilde{q}}$. Here, the function

$$f_{\gamma/e}(z,q^2) = \frac{\alpha}{2\pi} \frac{1 + (1 - z)^2}{z} \ln \frac{q^2}{m_e^2} \tag{30}$$

describes the effective photon distribution in $z \simeq p_\gamma/p_e$, $G(x,Q^2)$ denotes the gluon distribution in the proton and $\sigma(xzs)$ is the basic cross-section, eq.(27). Following ref. [6], we choose

$$Q^2 = \frac{q^2 - m_e^2}{\ln(q^2/m_e^2)} \tag{31}$$

as the gluon evolution scale with

$$q^2 = sx - (m_1 + m_2)^2 \tag{32}$$

characterizing the maximum virtuality of the photon.

Fig.7 shows the production cross-sections $\sigma(ep \to e\tilde{q}\bar{\tilde{q}}X)$ versus the squark mass $m_{\tilde{q}}$ for $\sqrt{s}$ = 1.4 and 1.8 TeV in comparison to the expectation at HERA. Again, precise estimates of the values of $m_{\tilde{q}}$ which can be reached in this channel must be left to a more detailed analysis. In particular, the heavy-quark backgrounds from $ep \to e\bar{t}tX$, $\nu\bar{t}bX$ require a careful study. Assuming that 100 $\tilde{q}\bar{\tilde{q}}$-events per year are sufficient to establish a signal, one would be able to detect squarks up to

$$\begin{aligned} m_{\tilde{q}} &\simeq 200 \text{ GeV} \quad \text{at } \sqrt{s} = 1.4 \text{ TeV}, \; L = 10^{32} \text{cm}^{-2}\text{s}^{-1}, \\ m_{\tilde{q}} &\simeq 150 \text{ GeV} \quad \text{at } \sqrt{s} = 1.8 \text{ TeV}, \; L = 10^{31} \text{cm}^{-2}\text{s}^{-1}. \end{aligned} \tag{33}$$

This, as we believe, reasonable guess indicates that $\tilde{e}q$ production gives access to considerably heavier squark masses than $\tilde{q}\bar{\tilde{q}}$ production, unless $m_{\tilde{I}} \gg m_{\tilde{q}}$ which is not expected in the usual models.

4. SQUARK-GLUINO PRODUCTION

Squarks and gluinos can be produced in ep collisions by photon-quark scattering as indicated by the diagrams shown in Fig.8. The integrated cross-section for $\gamma q \to \tilde{q}\tilde{g}$ reads [5]

$$\sigma(\hat{s}) = \frac{4\pi\alpha Q_q^2 \alpha_s(Q^2)}{3\hat{s}} \left[\beta (1 + 7\delta) - 4\delta(1 + \delta) \ln \frac{1 + \delta + \beta}{1 + \delta - \beta}\right] \tag{34}$$

where

$$\beta = \sqrt{1 - 2\frac{m_{\tilde{q}}^2 + m_{\tilde{g}}^2}{\hat{s}} + \delta^2}, \qquad \delta = \frac{m_{\tilde{q}}^2 - m_{\tilde{g}}^2}{\hat{s}}, \tag{35}$$

and where we have added $\tilde{q}_L$ and $\tilde{q}_R$ production taking $m_{\tilde{q}_L} = m_{\tilde{q}_R}$. The total cross-section for $ep \to e\tilde{q}\tilde{g}X$ is then obtained from eq.(34) and the Weizsäcker-William approximation described in eqs.(28-32). Evidently, in the formulas the gluon distribution $G(x,Q^2)$ is to be replaced by the sum of the quark distribution functions $\sum_q q(x,Q^2)$ and $m_{\tilde{q}}(m_{\tilde{g}})$ is to be substituted for $m_1(m_2)$.

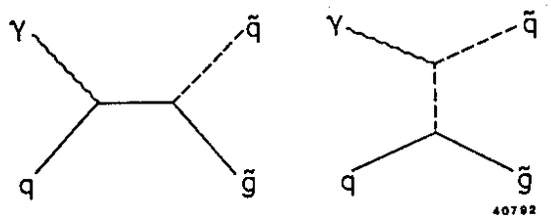

Fig.8 Diagrams contributing to $ep \to e\tilde{q}\tilde{g}X$.

The resulting cross-sections are plotted in Fig.9 versus $m_{\tilde{g}}$ for the two ep energies, $\sqrt{s}$ = 1.4 and 1.8 TeV, and for various values of $m_{\tilde{q}}$. It should be noted that the SUGRA relation $m_{\tilde{q}}^2 \simeq m_o^2 + 0.8\, m_{\tilde{g}}^2$ implied by eqs.(23) and (24) favours cross-sections on the left-hand side of the predictions for $m_{\tilde{q}} = m_{\tilde{g}}$ in Fig.9. If one takes the values of $m_{\tilde{q}}$ and $m_{\tilde{g}}$ corresponding to 100 $\tilde{q}\tilde{g}$-events per year as a rough estimate of the limits of observability for this process, similarly to the assumption made in eq.(33), one finds the following detection limits:

$$m_{\tilde{g}} \simeq 100\ (400)\ \text{GeV} \quad \text{for } m_{\tilde{q}} = 300\ (100)\ \text{GeV} \qquad (36)$$
$$\text{at } \sqrt{s} = 1.4\ \text{TeV},\ L = 10^{32}\text{cm}^{-2}\text{s}^{-1}\ ,$$

$$m_{\tilde{g}} \simeq 160\ (310)\ \text{GeV} \quad \text{for } m_{\tilde{q}} = 200\ (100)\ \text{GeV} \qquad (37)$$
$$\text{at } \sqrt{s} = 1.8\ \text{TeV},\ L = 10^{31}\text{cm}^{-2}\text{s}^{-1}\ .$$

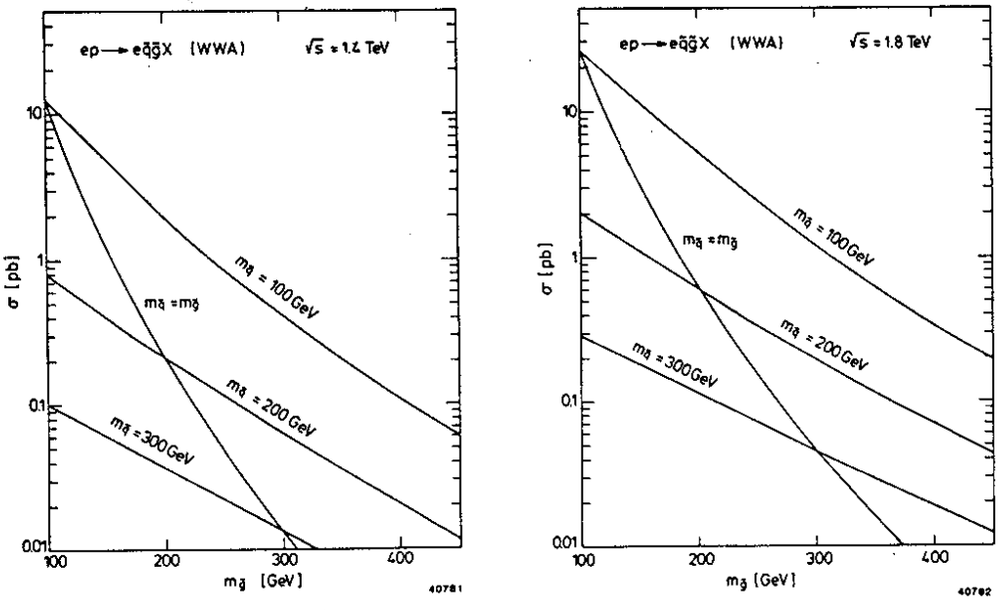

Fig.9 Squark-gluino production cross-sections for various assumptions on the squark mass.

Roughly speaking, if gluinos and squarks exist with masses in the range $m_{\tilde{g}} + m_{\tilde{q}} \lesssim$ (400-500) GeV, it should be possible to detect these sparticles at the LEP-LHC collider.

5. SLEPTON-GAUGINO PRODUCTION

As already pointed out in the introduction, searches for the processes $ep \to \tilde{l}\tilde{\chi} + X$ and $ep \to lq\tilde{\chi} + X$, $\tilde{\chi}$ denoting a chargino or neutralino state, are not expected to produce very useful limits. Here, we substantiate this claim by presenting an example, namely $ep \to \tilde{e}\tilde{\gamma}X$, which has been studied in detail in ref.[6]. This investigation was mainly motivated by the possibility that squarks could be so heavy that the processes discussed so far could not take place or would be strongly suppressed, while $\tilde{e}\tilde{\gamma}$ final states could still be produced if $m_{\tilde{e}} \ll m_{\tilde{q}}$ and $m_{\tilde{\gamma}} \approx 0$. Fig.10 shows the dominant diagrams contributing to $ep \to \tilde{e}\tilde{\gamma}X$ and Fig.11 illustrates the total cross-sections for $m_{\tilde{\gamma}} \approx 0$ and various values of $m_{\tilde{e}}$. We see that at $\sqrt{s} = 1.4$ TeV and $L = 10^{32}cm^{-2}s^{-1}$ selectron masses $m_{\tilde{e}} \gtrsim 150$ GeV are out of reach in this channel. The sensitivity at $\sqrt{s} = 1.8$ TeV and $L = 10^{31}cm^{-2}s^{-1}$ is even worse. Moreover, supposing $m_{\tilde{\gamma}} \approx 50$ (150) GeV one expects more events from $\tilde{e}\tilde{q}$ production if $m_{\tilde{q}} \lesssim 500$ (600) GeV as indicated by the results for model (a) shown in Figs.2 and 3.

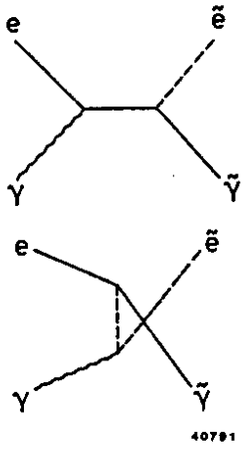

Fig.10 Diagrams contributing to $ep \to \tilde{e}\tilde{\gamma}X$.

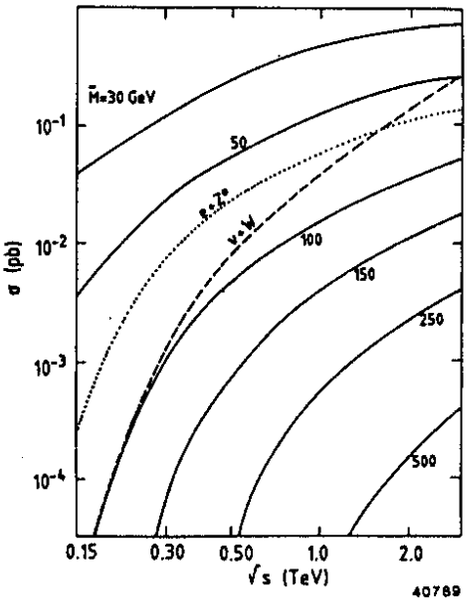

Fig.11 Selectron-photino production cross-sections for various values of the selectron mass $\tilde{M}$ assuming $m_{\tilde{\gamma}} = 0$. Also shown are the cross-sections ($\sigma \cdot B$) for the background processes $ep \to eZX$, $Z \to \nu\bar{\nu}$ and $ep \to \nu WX$, $W \to e\nu$. (from ref.[6])

6. SUMMARY

We have calculated total cross-sections for the production of the following sparticle final states in ep collisions:

$$\tilde{e}\tilde{q} + X,\ \tilde{\nu}\tilde{q} + X,\ e\tilde{q}\bar{\tilde{q}} + X,\ e\tilde{q}\tilde{g} + X,\ (\tilde{e}\tilde{\gamma} + X),$$

and have investigated the model-dependence of these predictions. Furthermore, we have assumed c.m. energies and luminosities which would be available in collisions of $e^{\mp}$ beams of LEP with a p beam of the LHC. From these studies we have then estimated detection limits for sparticles masses taking $\sigma(ep \to \tilde{e}\tilde{q}X,\ \tilde{e}\tilde{\gamma}X) = 0.01\ (0.1)$ pb and $\sigma(ep \to e\tilde{q}\bar{\tilde{q}}X,\ e\tilde{q}\tilde{g}X) = 0.1\ (1)$ pb as the smallest observable cross-sections at $\sqrt{s} = 1.4\ (1.8)$ TeV and $L = 10^{32}$ (10^{31}) $cm^{-2}s^{-1}$. This assumption is equivalent to requiring 10 events per year for final states in which a sparticle $(\tilde{e},\ \tilde{\gamma})$ emerges from the leptonic vertex, and 100 events per year if both sparticles are produced at the hadronic vertex. Obviously, one can expect a clearer signal from the first class of events than from the second kind.

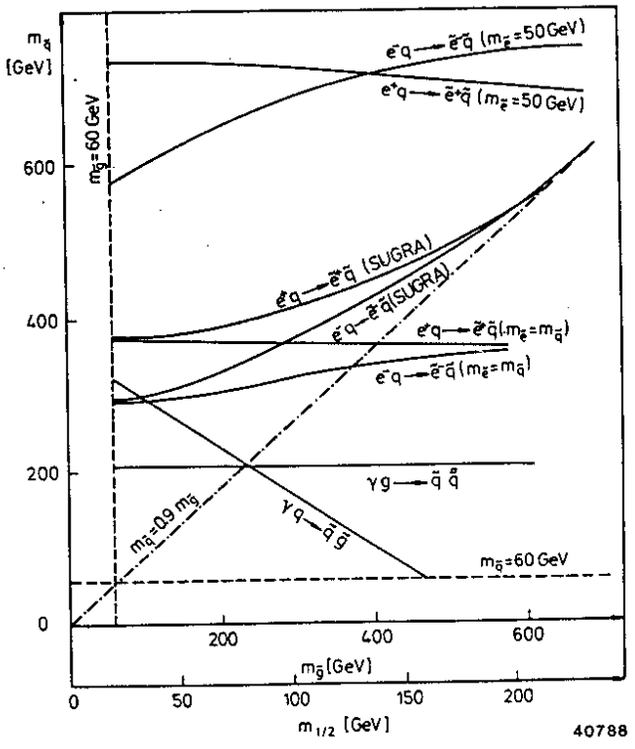

Fig.12 Summary of discovery limits expected at the LEP-LHC ep collider. Current bounds are indicated by dashed lines. Using the renormalization group relations (23) and (24) one has $m_{\tilde{q}} \gtrsim 0.9\ m_{\tilde{g}}$ (dashed-dotted line) and $m_{\tilde{g}} \simeq 3\ m_{1/2}$ (relation of horizontal scales).

Fig.12 summarizes our estimates of discovery limits. We see that the heaviest sparticle masses can be reached in pair-production of sleptons and squarks, although the individual detection limits depend crucially on the relation between $m_{\tilde{e}}$ and $m_{\tilde{q}}$ (and also to some extent on $m_{\tilde{g}}$ if supergravity mass relations are assumed). On the other hand, direct searches for gluinos produced in $ep \to e\tilde{q}\tilde{g}X$ are restricted to $m_{\tilde{g}} \lesssim 400$ GeV, while the squark masses accessible in $ep \to e\tilde{q}\tilde{g}X$ and in $ep \to e\tilde{q}\bar{\tilde{q}}X$ are limited to $m_{\tilde{q}} \lesssim 200$ GeV except for light gluinos. Finally, the bounds on charginos and neutralinos expected from the processes $ep \to \tilde{l}\tilde{\chi}X$ and $ep \to l\tilde{q}\tilde{\chi}X$ are not very interesting and are therefore not shown in Fig.12. However, it should be possible to extract some information on these states from a more detailed study of $ep \to \tilde{e}\tilde{q}X$ if a sufficiently strong signal is observed [4].

REFERENCES

[1] For reviews see
H.P. Nilles, Phys. Rep. 110 (1984) 1;
H.E. Haber and G.L. Kane, Phys. Rep. 117 (1985) 75.

[2] S.K. Jones and C.H. Llewellyn Smith, Nucl. Phys. B217 (1983) 145.

[3] P.R. Harrison, Nucl. Phys. B249 (1985) 704;
A. Bartl, H. Fraas and W. Majerotto, HEPHY-PUB 503/87;
J.A. Bagger and M.E. Peskin, Phys. Rev. D31 (1985) 2211 and Erratum D32 (1985) 1260;
G. Altarelli, B. Mele and R. Rückl, Proc. ECFA-CERN Workshop on a large Hadron Collider in the LEP Tunnel, Lausanne and CERN, 1984, ed. M. Jacob (ECFA 84/85, CERN 84-10, Geneva, 1984) p. 551.

[4] H. Komatsu and R. Rückl, DESY 87-088.

[5] M. Drees and K. Grassie, Z. Phys. C28 (1985) 451.

[6] G. Altarelli, G. Martinelli, B. Mele and R. Rückl, Nucl. Phys. B262 (1985) 204.

[7] P. Salati and J.C. Wallet, Phys. Lett. 122B (1983) 397.

[8] B.A. Campbell, J. Ellis and S. Rudaz, Nucl. Phys. B198 (1982) 1;
I. Antoniadis, C. Kounnas and R. Lacaze, Nucl. Phys. B211 (1983) 216;
C. Kounnas and D.A. Ross, Nucl. Phys. B214 (1983) 317;
L. Marleau, Phys. Rev. D32 (1985) 2928.

[9] M. Davier, Proc. of the XXIII. Int. Conf. on High Energy Physics, Berkeley, 1986, ed. S.C. Loken (World Scientific Publ. Co., Singapore, 1987) p. 25.

[10] E. Eichten, I. Hinchliffe, K. Lane and C. Quigg, Rev. Mod. Phys. 56 (1984) 579 and Erratum 58 (1986) 1065.

[11] G. Brianti, Proc. of the Workshop on Physics at Future Accelerators, La Thuile and CERN, 1987, ed. J.H. Mulvey (CERN 87-07, Geneva, 1987) Vol.I, p.6.

[12] J. Ellis and F. Pauss, Proc. of the Workshop on Physics at Future Accelerators, La Thuile and CERN, 1987, ed. J.H. Mulvey (CERN 87-07, Geneva, 1987) Vol.I, p.80.

[13] J. Ellis, Proc. of the Int. Symp. on Lepton and Photon Interactions at High Energies, Kyoto, 1985, eds. M. Konuma and K. Takahashi (Kyoto University, Kyoto, 1986) p.850;
E. Reya, Proc. of the XXIII. Int. Conf. on High Energy Physics, Berkeley, 1986, ed. S.C. Loken (World Scientific Publ. Co., Singapore, 1987) p.285.

[14] R.J. Cashmore et al., Phys. Rep. 122 (1985) 275.